Inorg. Chem. **2003**, *42*, 717−728

Structural and Spectroscopic Studies of Nickel(II) Complexes with a Library of Bis(oxime)amine-Containing Ligands

Michael J. Goldcamp, Sara E. Edison, Leah N. Squires, Dell T. Rosa, Neil K. Vowels, Nathan L. Coker, Jeanette A. Krause Bauer, and Michael J. Baldwin*

Department of Chemistry, University of Cincinnati, Cincinnati, Ohio 45221-0172

Received July 9, 2002

A library of tripodal amine ligands with two oxime donor arms and a variable coordinating or noncoordinating third arm has been synthesized, including two chiral ligands based on L-phenylalanine. Their Ni(II) complexes have been synthesized and characterized by X-ray crystallography, UV–vis absorption, circular dichroism, and FTIR spectroscopy, mass spectrometry, and room-temperature magnetic susceptibility. At least one crystal structure is reported for all but one Ni/ligand combination. All show a six-coordinate pseudo-octahedral coordination geometry around the nickel center, with the bis(oxime)amine unit coordinating in a facial mode. Three distinct structure types are observed: (1) for tetradentate ligands, six-coordinate monomers are formed, with anions and/or solvent filling out the coordination sphere; (2) for tridentate ligands, six-coordinate monomers are formed with $Ni^{II}(NO_3)_2$, with one monodentate and one bidentate nitrate filling the remaining coordination positions; (3) for tridentate ligands, six-coordinate, bis(μ-Cl) dimers are formed with $Ni^{II}Cl_2$, with one terminal and two bridging chlorides filling the coordination sphere. The UV–vis absorption spectra of the complexes show that the value of 10 Dq varies according to the nature of the third arm of the ligand. The trend based on the third arm follows the order alkyl/aryl < amide < carboxylate < alcohol < pyridyl < oxime.

Introduction

The development of new polydentate ligands is important for the discovery of new transition metal catalysts, for the advancement of bioinorganic chemistry both in its role of understanding the chemistry of metallobiomolecules and in producing useful new biomimetic and bioinspired reactions, and for the continuing development of basic coordination chemistry. In particular, the design of a series of polydentate ligands combining a common unit with a systematically variable feature provides the opportunity to examine the effect of that variation on the chemistry and spectroscopy of the metal complexes of the ligand series and to optimize any useful chemistry that is observed in those complexes. The series of new polydentate ligands described here uses a "tripodal amine" type motif. The common unit is an "N_3" donor set consisting of an amine with a pair of oxime-containing arms, and the third arm off the tertiary amine provides the variable feature. It may contribute a strong donor, weak donor, or nondonor group. Variation of the third arm may be used to modify the electronic structure of the metal complex, the environment around the metal center (steric, hydrophobic or polar properties, hydrogen bonding propensity, etc.), and the solubility properties. All of these properties are useful in optimizing potential catalysts. From a bioinorganic viewpoint, oximes are not known to be present as ligands in metalloproteins, although oxime-containing tetrapeptides with antibacterial, cytotoxic, or anti-inflammatory activity have been found in marine sponges.[1] Also, the enzyme ammonia monooxygenase produces hydroxylamine,[2] which forms oximes upon reaction with aldehydes or ketones. Thus, incorporation of oximes in post-translationally modified proteins is not unreasonable from a biosynthetic standpoint. However, an exact match of the donor groups is not necessary for useful bioinorganic modeling, as has been shown on numerous occasions by the use of pyridyl, pyrazolyl, and macrocyclic polyamine ligands in place of the imidazole group of histidine in bioinorganic model complexes.

* Author to whom correspondence should be addressed. E-mail: michael.baldwin@uc.edu.

(1) Franklin, M. A.; Penn, S. G.; Lebrilla, C. B.; Lam, T. H.; Pessah, I. N.; Molinski, T. F. *J. Nat. Prod.* **1996**, *59*, 1121−1127.

(2) (a) Hollocher, T. C.; Tate, M. E.; Nicholas, D. J. D. *J. Biol. Chem.* **1981**, *256*, 10834−10836. (b) Hooper, A. B.; Vannelli, T.; Bergmann, D. J.; Arciero, D. M. *Antoine van Leeuwenhoek* **1997**, *71*, 59−67.

10.1021/ic025860q CCC: $25.00
Published on Web 01/04/2003

The protonation state of the oximes significantly alters their ligand properties, and deprotonation is easily accomplished by addition of hydroxide or some weaker bases. Ligands containing multiple oximate (deprotonated oxime) donor groups have been shown to stabilize unusually highly valent transition metals, such as Ni(III) and Ni(IV).[3] We have recently reported the structural and electrochemical characterization and reactivity of the Ni(II) complexes of the tris(oxime) containing ligand tris(1-propan-2-onyl oxime)amine (herein designated $TRISOXH_3$, previously designated Ox_3H_3) in various protonation states.[4] The Ni(II)−oximate complex reacts with O_2 to oxidize Ph_3P to Ph_3PO, with incorporation of oxygen from O_2. This unusual reactivity between Ni(II) and O_2 is due in part to the significant lowering of the Ni(II) oxidation potentials by the polyoximate donor set. It is anticipated that variation of the third arm of the ligand, while maintaining the basic bis(oxime)amine donor set, will allow the O_2 reactivity of the Ni(II) complexes to be optimized by modulation of the electronic structure of the metal through variation of the donor properties of the ligand and by modifying the interaction of the active metal complex with potential oxidation substrates.

In this paper, we report the synthesis and characterization of a series of new tripodal amine ligands containing two oxime arms and a variable third arm. We also report the structural characterization of the Ni(II) complexes of these ligands in the neutral oxime protonation state. The structures obtained to date allow prediction of additional structures as the ligand library is expanded. For the tridentate ligands in particular (those in which the third ligand arm is a nondonor alkyl or aryl group), complexes derived from $NiCl_2$ and $Ni(NO_3)_2$ have very different but predictable structure types. Spectroscopic studies of the series of complexes show that the ligand variation produces a reasonably predictable spectrochemical series for the Ni(II) ligand field transitions, based on the nature of the group on the third arm.

Experimental Section

Materials. All chemicals were obtained from Fisher/Acros or Aldrich and used without further purification. The preparations of the TACO reagent (the triethylamine adduct of chloroacetone oxime),[5] glycine *N*′-methylamide,[6] L-phenylalanine *N*′-methylamide,[7] bromoacetophenone oxime,[8] tris(1-propan-2-onyl oxime)amine,[4,9] and nickel(II) (tris(1-propan-2-onyl oxime)amine) nitrate[4] have been previously reported. Purity of the synthesized ligands is demonstrated by their ^{1}H NMR spectra. Elemental analysis (CHN) is reported on bulk solids for those complexes for which X-ray crystallographic structural characterization is reported to demonstrate that the structures are representative of the bulk material. For all others, mass spectral data are used to confirm the complex formulation.

Ligand Syntheses. *N*-*n*-Propyl-*N*,*N*-bis(1-propan-2-onyl oxime)-amine ($PRABOH_2$). TACO (3.4 g, 1.6×10^{-2} mol) and *n*-propylamine (0.48 g, 8.1×10^{-3} mol) were combined in acetonitrile (125 mL), and the mixture was heated to reflux. After approximately 30 min, almost all TACO had dissolved. The reaction was heated an additional 30 min, and the small amount of unreacted TACO was filtered from the mixture. The filtrate solvent was removed by rotary evaporation to give an orange crude solid. The crude solid was extracted with diethyl ether (200 mL), and the ether was removed by rotary evaporation to give a gold-colored oil. The oil was washed with hexanes (100 mL) and dried under vacuum, giving a pale orange solid, which was washed with three 10 mL portions of cold water to give the off-white solid product (0.97 g, 4.8×10^{-3} mol, 59% yield). ^{1}H NMR (d_6-DMSO): 0.81 (t, 3H), 1.41 (q, 2H), 1.76 (s, 6H), 2.26 (t, 2H), 2.94 (s, 4H), 10.50 (s, 2H) ppm. ^{13}C NMR (d_6-DMSO): 11.60, 12.07, 19.20, 54.80, 57.76, 154.05 ppm. FTIR (KBr): 2965 (s), 2926 (s), 2876 (s), 2827 (s), 1664 (w), 1463 (m), 1442 (m), 1386 (w), 1366 (m), 1269 (m), 1256 (w), 1176 (w), 1137 (w), 1046 (m), 1022 (m), 966 (s), 937 (m), 913 (w), 858 (w), 827 (w), 750 (w), 677 (w) cm^{-1}. Mp 69−73 °C. MS: $(M + Na)^+$ at $m/z = 224.1$ (100%), $(M + H)^+$ at $m/z = 202.2$ (30%).

***N*,*N*-Bis(1-propan-2-onyl oxime) Glycine *N*′-Methylamide ($GLABOH_3$).** TACO (3.8 g, 1.8×10^{-2} mol) and glycine *N*′-methylamide (0.80 g, 9.1×10^{-3} mol) were combined in acetonitrile (50 mL), and the mixture was heated to reflux. After approximately 1 h, almost all TACO had dissolved. The reaction was heated for an additional 2 h at approximately 40 °C, resulting in a pale orange solution. The solvent was removed by rotary evaporation to yield a crude orange solid. The solid was extracted with diethyl ether (100 mL), and the ether was allowed to slowly evaporate to give an off-white solid. Washing with THF (<10 mL) removed some color to give a nearly white solid (0.32 g, 1.4×10^{-3} mol, 16% yield). ^{1}H NMR (d_6-DMSO): 1.78 (s, 6H), 2.60 (d, 3H), 2.96 (s, 2H), 3.08 (s, 4H), 7.54 (q, 1H), 10.59 (s, 2H) ppm. ^{13}C NMR (d_6-DMSO): 12.32, 25.32, 56.19, 58.14, 153.58, 170.24 ppm. FTIR (KBr): 3276 (s, br), 3082 (m, br), 2878 (s), 2838 (s), 1651 (vs), 1548 (m), 1489 (m), 1435 (m), 1405 (m), 1366 (m), 1340 (w), 1265 (m), 1164 (w), 1131 (w), 1031 (m), 962 (m), 913 (m), 890 (m), 821 (w) cm^{-1}. Mp 119−124 °C (dec). MS: $(M + Na)^+$ at $m/z = 253.1$ (100%), $(M + H)^+$ at $m/z = 231.1$ (15%).

***N*-Phenethyl-*N*,*N*-bis(1-propan-2-onyl oxime)amine ($PEABOH_2$).** $PEABOH_2$ was prepared similarly to $PRABOH_2$ using TACO (10.0 g, 4.79×10^{-2} mol) and phenethylamine (2.9 g, 2.4×10^{-2} mol). The product (4.9 g, 1.9×10^{-2} mol, 79% yield) was further purified by recrystallization from boiling water, with methanol added dropwise until all of the solid dissolved, followed by slow cooling to room temperature. ^{1}H NMR (d_6-DMSO): 1.67 (s, 6H), 2.56 (t, 2H), 2.71 (t, 2H), 3.03 (s, 4H), 7.13−7.29 (m, 5H), 10.53 (s, 2H) ppm. ^{13}C NMR ($CDCl_3$): 12.28, 32.87, 55.59, 57.90, 125.98, 128.31, 128.77, 140.08, 157.15 ppm. FTIR (KBr): 2951 (s), 2830 (s), 1939 (w), 1863 (w), 1798 (w), 1660 (w), 1600 (w), 1443 (s), 1369 (s), 1259 (m), 1130 (m), 1022 (s), 962 (s), 935 (s), 829 (m), 748 (s), 695 (s), 582 (m) cm^{-1}. Mp 94−98 °C. MS: $(M + H)^+$ at $m/z = 264$ (100%).

(3) (a) Baucom, E. I.; Drago, R. S. *J. Am. Chem. Soc.* **1971**, *93*, 6469−6475. (b) Korvenranta, J.; Saarinen, H.; Nasakkala, M. *Inorg. Chem.* **1982**, *21*, 4296−4300. (c) Singh, A. N.; Singh, R. P.; Mohanty, J. G.; Chakravorty, A. *Inorg. Chem.* **1977**, *16*, 2597−2601. (d) Singh, A. N.; Chakravorty, A. *Inorg. Chem.* **1980**, *19*, 969−971. (e) Sproul, G.; Stucky, G. D. *Inorg. Chem.* **1973**, *12*, 2898−2901.

(4) Goldcamp, M. J.; Robison, S. E.; Krause Bauer, J. A.; Baldwin, M. J. *Inorg. Chem.* **2002**, *41*, 2307−2309.

(5) Goldcamp, M. J.; Rosa, D. T.; Landers, N. A.; Mandel, S. M.; Krause Bauer, J. A.; Baldwin, M. J. *Synthesis* **2000**, *14*, 2033−2038.

(6) Marvel, C. S.; Elliott, J. R.; Boettner, F. E.; Yuska, H. *J. Am. Chem. Soc.* **1946**, *68*, 1681−1686.

(7) Nowick, J. S.; Holmes, D. L.; Noronha, G.; Smith, E. M.; Nguyen, T. M.; Huang, S.-L. *J. Org. Chem.* **1996**, *61*, 3929−3934.

(8) Barton, D. H. R.; Crich, D.; Kretzschmar, G. *J. Chem. Soc., Perkin Trans. 1* **1986**, 39−54.

(9) (a) Matthaiopoulos, G. *Chem. Ber.* **1898**, *31*, 2396. (b) Ogloblin, K. A.; Potekhin, A. A. *J. Org. Chem. USSR (Engl. Transl.)* **1965**, *1*, 399−405. (c) Goldcamp, M. J.; Krause Bauer, J. A.; Baldwin, M. J. *Acta Crystollogr., Sect. E.* **2002**, *E58*, 1354−1355.

***N*-Phenyl-*N*,*N*-bis(1-propan-2-onyl oxime)amine ($ABOH_2$).** $ABOH_2$ was prepared similarly to $PRABOH_2$, using aniline (2.2 g, 2.4×10^{-2} mol) and TACO (10 g, 4.8×10^{-2} mol) in 150 mL of acetonitrile. The product was purified by dropwise rinsing with dichloromethane to give white solid $ABOH_2$ (0.82 g, 4.2×10^{-3} mol, 18% yield). Further purification can be achieved by dissolution in a minimal volume of ethyl acetate, followed by slow diffusion of a layer of hexane (about four times the volume of ethyl acetate) in a closed test tube for several days. ^{1}H NMR (d_6-DMSO): 1.70 (s, 6H), 4.02 (s, 4H), 6.61 (t, 1H), 6.79 (d, 2H), 7.11 (t, 2H), 10.61 (s, 2H) ppm. ^{13}C NMR (d_6-DMSO): 11.81, 54.85, 112.90, 116.57, 128.98, 148.85, 154.13 ppm. FTIR (KBr): 3273 (s), 2913 (m), 1935 (w), 1832 (w), 1600 (s), 1504 (s), 1391 (s), 1260 (w), 1226 (s), 1187 (m), 1011 (s), 958 (m), 825 (m), 756 (s), 675 (s), 571 (m), 508 (m), 420 (w) cm^{-1}. Mp 138−146 °C. MS: $(M + Na)^+$ at $m/z = 258.1$ (100%), $(M + H)^+$ at $m/z = 236.1$ (10%).

***N*-(Pyridin-2-yl)methyl-*N*,*N*-bis(1-propan-2-onyl oxime)amine ($PYRABOH_2$).** $PYRABOH_2$ was prepared similarly to $PRABOH_2$, using TACO (4.3 g, 2.1×10^{-2} mol) and 2-(aminomethyl)-pyridine (1.0 g, 9.2×10^{-3} mol). The product (0.71 g, 2.8×10^{-3} mol, 34% yield) was purified by recrystallization from boiling water, with methanol added dropwise until all of the solid dissolved, followed by slow cooling to room temperature. ^{1}H NMR (d_6-acetone): 1.87 (s, 6H), 3.07 (s, 4H), 3.66 (s, 2H), 7.23 (t, 1H), 7.51 (d, 1H), 7.76 (t, 1H), 8.49 (d, 1H), 9.77 (s, 2H) ppm. ^{13}C NMR (d_6-acetone): 12.29, 58.62, 60.14, 122.87, 123.73, 137.18, 149.67, 155.28, 160.26 ppm. FTIR (KBr): 2926 (s), 2874 (s), 2828 (s), 2816 (s), 2708 (m), 1681 (w), 1638 (w), 1617 (w), 1596 (s), 1573 (m), 1476 (s), 1438 (s), 1368 (s), 1267 (m), 1246 (m), 1054 (m), 1034 (s), 1003 (m), 989 (m), 973 (m), 960 (m), 925 (s) 820 (m), 777 (m), 735 (m), 669 (m), 623 (m) cm^{-1}. Mp 96−102 °C. MS: $(M + Na)^+$ at $m/z = 273$ (100%).

***N*,*N*-Bis(1-propan-2-onyl oxime) L-Phenylalanine *N*′-Methylamide ($PAMBOH_3$).** TACO (3.5 g, 1.7×10^{-2} mol) and L-phenylalanine *N*′-methylamide (1.4 g, 7.9×10^{-3} mol) were combined in 100 mL of 2-propanol, and the reaction mixture was heated to reflux and stirred for 4 h, after which the solvent was removed by rotary evaporation. The crude product was extracted with two 200 mL portions of diethyl ether, and the ether was evaporated to yield an oil, which was dried under vacuum to yield a white solid (0.49 g, 1.5×10^{-3} mol, 19% yield). The solid $PAMBOH_3$ can be further purified by slow diffusion of hexane into an ethyl acetate solution of $PAMBOH_3$. ^{1}H NMR (d_6-DMSO): 1.58 (s, 6H), 1.71 (m, 2H), 2.55 (d, 3H), 2.68 (m, 1H), 2.90 (s, 4H), 7.20−7.24 (m, 5H), 7.56 (d, 1H), 10.56 (s, 2H) ppm. ^{13}C NMR (d_6-DMSO): l2.19, 25.56, 32.66, 54.26, 64.17, 126.02, 128.13, 129.28, 139.40, 154.40, 183.12 ppm. FTIR (KBr): 2923 (m), 1955 (w), 1654 (vs), 1550 (s), 1451 (s), 1412 (s), 1379 (s), 1260 (m), 1157 (m), 1128 (m), 1034 (m), 954 (m), 747 (m), 701 (m), 494 (w) cm^{-1}. Mp 44−52 °C. MS: $(M + H)^+$ at $m/z = 321$ (100%).

***N*,*N*-Bis(1-acetophenone oxime) L-Phenylalanine *N*′-Methylamide ($PAMABPOH_3$).** TABO (vide infra) (0.724 g, 2.30×10^{-3} mol) and L-phenylalanine *N*′-methylamide (0.207 g, 1.16×10^{-3} mol) were combined in 50 mL of 2-propanol, and the mixture was heated to reflux and stirred for 3 h. The solvent was then removed by rotary evaporation to yield a crude solid, which was extracted with two 40 mL portions of diethyl ether. The ether extracts were then evaporated to give a yellow oil, which was dried under vacuum to yield a white solid, $PAMABPOH_3$ (0.154 g, 3.47×10^{-4} mol, 30% yield). ^{1}H NMR (d_6-DMSO): 2.28 (d, 3H), 3.03 (m, 1H), 3.61 (m, 4H), 3.91 (m, 2H), 6.38 (m, 1H), 7.03−7.41 (m, 15H), 11.05 (s, 1H), 11.63 (s, 1H) ppm. ^{13}C NMR (d_6-DMSO): 25.35, 31.43, 43.74, 54.32, 62.23, 64.22, 125.85, 126.82, 127.63, 127.92, 128.12, 128.46, 128.89, 129.32, 132.48, 135.64, 139.69, 152.85, 154.51, 170.75 ppm. FTIR (KBr): 3057 (s), 2968 (s), 2880 (s), 1957 (w), 1891 (w), 1814 (w), 1655 (vs), 1537 (m), 1495 (s), 1441 (s), 1412 (s), 1300 (m), 1258 (m), 1159 (w), 1125 (m), 1073 (w), 1001 (s), 936 (s), 751 (s), 699 (vs), 643 (m), 540 (w) cm^{-1}. Mp 72−78 °C. MS: $(M + Na)^+$ at $m/z = 467.2$ (100%).

***N*-*n*-Octyl-*N*,*N*-bis(1-propan-2-onyl oxime)amine ($OBOH_2$).** $OBOH_2$ was prepared in a manner similar to $PRABOH_2$, using TACO (10.1 g, 4.82×10^{-2} mol) and *n*-octylamine (3.1 g, 2.4×10^{-2} mol). $OBOH_2$ is a golden oil (2.1 g, 7.7×10^{-3} mol, 32% yield). ^{1}H NMR ($CDCl_3$): 0.80 (3H, t), 1.18 (m, br, 10H), 1.35 (m, br, 2H), 1.83 (s, 6H), 2.30 (t, 2H), 2.96 (s, 4H), 9.53 (s, br, 2H) ppm. ^{13}C NMR ($CDCl_3$): 12.08, 13.75, 18.61, 22.32, 26.50, 26.96, 29.15, 31.52, 53.72, 57.72, 156.91 ppm. FTIR (KBr): 3160 (s), 2926 (s), 2855 (m), 1511 (vs), 1346 (vs), 1265 (s), 1076 (m), 1020 (m), 688 (m) cm^{-1}. MS: $(M + Na)^+$ at $m/z = 294.2$ (90%), $(M + H)^+$ at $m/z = 272.2$ (100%).

Potassium *N*,*N*-Bis(1-propan-2-onyl oxime) Glycinate ($GLYBOH_2K$). TACO (3.50 g, 1.68×10^{-2} mol) and glycine ethyl ester hydrochloride (1.00 g, 7.16×10^{-3} mol) were added together in 200 mL of 2-propanol, and the mixture was heated to reflux and stirred. A solution of triethylamine (0.725 g, 7.16×10^{-3} mol) in 20 mL of 2-propanol was added dropwise over a period of about 30 min. The reaction was heated an additional 1.5 h, after which the solvent was removed by rotary evaporation to yield a crude solid. A 200 mL portion of diethyl ether was added to the crude solid, and the mixture was stirred for 1 h. The mixture was then filtered, and the ether was evaporated to yield an oil, which was washed with hexane and dried under vacuum. The oil was then dissolved in a minimal amount of ethyl acetate, and the solution was run through a 6 cm long silica gel column. The orange-colored materials did not move from the top of the column, and the pale yellow and colorless fractions were collected and dried to yield 1.41 g of a white solid, *N*,*N*-bis(1-propan-2-onyl oxime) glycine ethyl ester. A portion of this product (0.20 g, 8.1×10^{-4} mol) was dissolved in 15 mL of 50/50 methanol/water, and 0.80 mL of a 1.0 M KOH (in methanol) solution was added dropwise over 30 min. The solution was heated at 50 °C for several hours and then stirred overnight at room temperature. The solvent was then removed by rotary evaporation, yielding an off-white solid. This solid was washed with 200 mL of diethyl ether (to remove any unreacted ester starting material) to give a white solid, $GLYBOH_2K$ (0.137 g, 5.4×10^{-4} mol, 66% yield). The product was used without further purification. ^{1}H NMR (D_2O): 1.73 (s, 6H), 2.07 (s, 4H), 2.69 (s, 2H), 10.45 (s, br, 2H) ppm. ^{13}C NMR (D_2O): 12.69, 58.00, 58.33, 159.35, 178.88 ppm. FTIR (KBr): 2909 (s), 1580 (vs), 1497 (w), 1457 (w), 1394 (m), 1310 (m), 1263 (w), 1156 (w), 1124 (w), 1044 (m), 959 (w), 928 (m), 743 (m), 678 (w) cm^{-1}. Mp 196−206 °C (dec). MS: $(M - K)^-$ at $m/z = 216$ (85%).

***N*-2-Hydroxyethyl-*N*,*N*-bis(1-propan-2-onyl oxime)amine ($EABOH_3$).** $EABOH_3$ was prepared similarly to $PRABOH_2$, using TACO (5.0 g, 2.4×10^{-2} mol) and ethanolamine (0.70 g, 1.1×10^{-2} mol). $EABOH_3$ (1.6 g, 7.9×10^{-3} mol, 72% yield) was further purified by dissolution in a minimal volume of ethyl acetate, followed by slow diffusion of a layer of hexane (about four times the volume of ethyl acetate) in a closed test tube for several days. ^{1}H NMR (d_6-DMSO): 0.82 (s, 6H), 1.49 (t, 2H), 2.08 (s, 4H), 2.51 (m, 2H), 9.56 (s, 2H) ppm. ^{13}C NMR (d_6-DMSO): 12.36, 55.59, 58.61, 59.15, 154.54 ppm. FTIR (KBr): 2919 (s), 2875 (s), 2815 (s), 1675 (w), 1493 (m), 1445 (m), 1380 (m), 1272 (m), 1219 (w), 1135 (w), 1081 (m), 1039 (s), 966 (s), 780 (m), 671 (m) cm^{-1}. Mp

120−128 °C. MS: $(M_2 + Na)^+$ at $m/z = 429.2$ (60%), $(M + Na)^+$ at $m/z = 226.1$ (100%), $(M + H)^+$ at $m/z = 204.1$ (10%).

***N,N,N*-Trimethyl-*N*-(1-acetophenone oxime)ammonium Bromide (TABO).** A solution of triethylamine (0.20 g, 2.0×10^{-3} mol) in diethyl ether (10 mL) was added to a stirring solution of bromoacetophenone oxime (0.37 g, 1.7×10^{-3} mol) in diethyl ether (10 mL). A white precipitate immediately formed, and after 10 min of stirring, the mixture was filtered to yield a white solid, *N*,*N*,*N*-trimethyl-*N*-(1-acetophenone oxime)ammonium bromide (0.42 g, 1.3×10^{-3} mol, 76% yield), which was used without further purification. ^{1}H NMR (d_6-DMSO): 1.11 (t, 9H), 3.21 (q, 6H), 4.43 (s, 2H), 7.46 (m, 4H), 7.63 (d, 1H), 7.75 (s, 1H) ppm. FTIR (KBr): 3086 (s), 2994 (s), 2811 (m), 1622 (w), 1481 (s), 1406 (s), 1294 (m), 1158 (m), 1074 (w), 1028 (s), 1003 (s), 949 (m), 902 (w), 793 (s), 766 (s), 702 (s), 531 (w) cm^{-1}.

Nickel(II) Complexes. Nickel(II) (Tris(1-propan-2-onyl oxime)-amine) Chloride ($Ni(TRISOXH_3)Cl_2$). Tris(1-propan-2-onyl oxime)-amine ($TRISOXH_3$, 0.20 g (8.7×10^{-4} mol)) and 0.21 g (8.8×10^{-4} mol) nickel(II) chloride hexahydrate were added together in about 15 mL of methanol and stirred to yield a blue solution, which gave a blue solid (0.26 g, 7.2×10^{-4} mol, 82% yield) after slow evaporation of the solvent. Blue crystals for X-ray crystallography were obtained by slow evaporation of a methanol/ethyl acetate solution of $Ni(TRISOXH_3)Cl_2$ in a test tube. FTIR (KBr): 1662 (w), 1632 (w), 1466 (s), 1434 (s), 1387 (s), 1292 (w), 1237 (m), 1117 (w), 1072 (s), 1029 (s), 940 (m), 872 (w), 848 (w) 656 (m) cm^{-1}. MS: $Ni(TRISOXH_3)Cl^+$ at $m/z = 323$ (100%). Anal. Calcd for $Ni(C_9H_{18}N_4O_3)Cl_2$ (359.86): C, 30.04; H, 5.04; N, 15.57. Found: C, 30.12; H, 4.63; N, 15.41.

Nickel(II) (*N*-*n*-Propyl-*N,N*-bis(1-propan-2-onyl oxime)amine) Nitrate ($Ni(PRABOH_2)(NO_3)_2$). *N*-*n*-Propyl-*N*,*N*-bis(1-propan-2-onyl oxime)amine (0.20 g (9.9×10^{-4} mol)) ($PRABOH_2$) and 0.29 g (1.0×10^{-3} mol) of nickel(II) nitrate hexahydrate were added together in about 15 mL of methanol and stirred to yield a blue solution, which after evaporation of the solvent yielded a blue solid (0.16 g, 4.2×10^{-4} mol, 62% yield). Blue crystals for X-ray crystallography were obtained by slow evaporation of a methanol/ethyl acetate/acetone solution of $Ni(PRABOH_2)(NO_3)_2$. FTIR (KBr): 2970 (m), 2938 (m), 1500 (s), 1464 (s), 1448 (s), 1375 (s), 1318 (s), 1265 (m), 1110 (w), 1072 (m), 1043 (m), 941 (m), 851 (w), 814 (w), 750 (w), 685 (w), 579 (w) cm^{-1}. MS: $Ni(PRABOH_1)^+$ at $m/z = 258.1$ (50%), $Ni(PRABOH_1)(CH_3OH)^+$ at $m/z = 290.1$ (65%), $Ni(PRABOH_2)NO_3^+$ at $m/z = 321.1$ (90%). Anal. Calcd for $Ni(C_9H_{19}N_3O_2)(NO_3)_2$ (208.73): C, 28.15; H, 4.99; N, 18.24. Found: C, 28.19; H, 4.55; N, 18.10.

Nickel(II) (*N*-*n*-Propyl-*N,N*-bis(1-propan-2-onyl oxime)amine) Chloride ($[Ni(PRABOH_2)Cl]_2(\mu\text{-}Cl)_2$). $[Ni(PRABOH_2)Cl]_2(\mu\text{-}Cl)_2$ was prepared similarly to $Ni(TRISOXH_3)Cl_2$ in methanol. Green crystals (73% yield) for X-ray crystallography were obtained by slow evaporation of an acetone solution of $[Ni(PRABOH_2)Cl]_2(\mu\text{-}Cl)_2$ in a test tube. FTIR (KBr): 2961(m), 2876 (m), 1660 (m), 1604 (w), 1465 (s), 1371 (s), 1292 (w), 1245 (m), 1235 (m), 1112 (m), 1064 (s), 1033 (m), 992 (w), 939 (m), 852 (m), 674 (m), cm^{-1}. MS: $[Ni(PRABOH_2)]_2Cl_3^+$ at $m/z = 623$ (35%), $Ni(PRABOH_2)Cl^+$ at $m/z = 294$ (100%) Anal. Calcd for $Ni(C_9H_{19}N_3O_2)Cl_2 \cdot 1H_2O$ (348.88): C, 30.98; H, 6.07; N, 12.04. Found: C, 31.46; H, 5.86; N, 11.73.

Nickel(II) (*N*-Phenethyl-*N,N*-bis(1-propan-2-onyl oxime)-amine) Chloride ($[Ni(PEABOH_2)Cl]_2(\mu\text{-}Cl)_2$). $[Ni(PEABOH_2)Cl]_2(\mu\text{-}Cl)_2$ was prepared similarly to $Ni(TRISOXH_3)Cl_2$ in methanol. Green crystals (71% yield) for X-ray crystallography were obtained by slow evaporation of a methanol/ethyl acetate solution of $[Ni(PEABOH_2)Cl]_2(\mu\text{-}Cl)_2$ in a test tube. FTIR (KBr): 2901 (m), 1456 (vs), 1423 (s), 1373 (m), 1240 (m), 1109 (m), 1073 (s), 1024 (m), 934 (m), 850 (m), 750 (m), 702 (m), 680 (m), 610 (m), 590 (m), 512 (m) cm^{-1}. MS: $[Ni(PEABOH_2)]_2Cl_3^+$ at $m/z = 749.1$ (100%). Anal. Calcd for $Ni(C_{14}H_{21}N_3O_2)Cl_2$ (368.91): C, 42.79; H, 5.39; N, 10.69. Found: C, 42.61; H, 5.24; N, 10.60.

Nickel(II) (*N*-Phenethyl-*N,N*-bis(1-propan-2-onyl oxime)-amine) Nitrate ($Ni(PEABOH_2)(NO_3)_2$). $Ni(PEABOH_2)(NO_3)_2$ was prepared similarly to $Ni(PRABOH_2)(NO_3)_2$ in methanol, yielding a blue solid (57% yield). FTIR (KBr): 3161 (w), 2929 (w), 1494 (m), 1454 (m), 1384 (vs), 1338 (w), 1272 (m), 1243 (w), 1106 (w), 1077 (w), 1020 (w), 929 (w), 855 (w), 748 (m), 688 (m), 519 (m) cm^{-1}. MS: $Ni(PEABOH_2)NO_3^+$ at $m/z = 383.1$ (95%).

Nickel(II) (*N*-*n*-Octyl-*N,N*-bis(1-propan-2-onyl oxime)amine) Chloride ($[Ni(OBOH_2)Cl]_2(\mu\text{-}Cl)_2$). $[Ni(OBOH_2)Cl]_2(\mu\text{-}Cl)_2$ was prepared similarly to $Ni(TRISOXH_3)Cl_2$ in acetonitrile, yielding a green solid (55% yield). Green crystals for X-ray crystallography were obtained by slow evaporation of an acetone/diethyl ether solution of $[Ni(OBOH_2)Cl]_2(\mu\text{-}Cl)_2$ in a test tube. FTIR (KBr): 2954 (m), 2927 (s), 2855 (s), 1628 (w), 1464 (s), 1432 (m), 1373 (m), 1343 (w), 1288 (w), 1241 (m), 1232 (m), 1113 (m), 1078 (m), 1052 (m), 1035 (m), 994 (w), 932 (m), 851 (m), 724 (w), 689 (m), 680 (m), 661 (m), 588 (m) cm^{-1}. MS: $[Ni(OBOH_2)]_2Cl_3^+$ at $m/z = 763$ (30%), $Ni(OBOH_2)Cl^+$ at $m/z = 364$ (100%). Anal. Calcd for $Ni(C_{14}H_{29}N_3O_2)Cl_2$ (401.00): C, 41.93; H, 7.29; N, 10.48. Found: C, 42.06; H, 7.17; N, 10.38.

Nickel(II) (*N*-*n*-Octyl-*N,N*-bis(1-propan-2-onyl oxime)amine) Nitrate ($Ni(OBOH_2)(NO_3)_2$). $Ni(OBOH_2)(NO_3)_2$ was prepared similarly to $Ni(PRABOH_2)(NO_3)_2$ in methanol, yielding a blue solid (48% yield). FTIR (KBr): 2956 (s), 2926 (s), 2855 (m), 1678 (w), 1612 (w), 1508 (s), 1439 (s), 1385 (s), 1346 (s), 1265 (s), 1111 (w), 1076 (m), 1058 (m), 1020 (m), 926 (w), 852 (w), 814 (w), 753 (w), 723 (w), 688 (m), 581 (w) cm^{-1}. MS: $[Ni(OBOH_1)]_2NO_3^+$ at $m/z = 718.3$ (30%), $Ni(OBOH_2)NO_3^+$ at $m/z = 391.1$ (100%).

Nickel(II) (*N*-Phenyl-*N,N*-bis(1-propan-2-onyl oxime)amine) Nitrate ($Ni(ABOH_2)(NO_3)_2$). $Ni(ABOH_2)(NO_3)_2$ was prepared similarly to $Ni(PRABOH_2)(NO_3)_2$ in methanol. Blue crystals (70% yield) for X-ray crystallography were obtained by slow evaporation of an acetone solution of $Ni(ABOH_2)(NO_3)_2$ in a flask. FTIR (KBr): 2932 (m), 1595 (m), 1500 (s), 1456 (s), 1374 (s), 1317 (s), 1269 (s), 1235 (m), 1183 (m), 1078 (m), 1045 (m), 1023 (m), 924 (m), 859 (w), 823 (w), 789 (m), 756 (m), 681 (m), 550 (w) cm^{-1}. MS: $[Ni(ABOH_1)]_2NO_3^+$ at $m/z = 646$ (30%), $Ni(ABOH_2)NO_3^+$ at $m/z = 355$ (50%), $Ni(ABOH_1)^+$ at $m/z = 292$ (30%). Anal. Calcd for $Ni(C_{12}H_{17}N_3O_2)(NO_3)_2$ (417.99): C, 34.48; H, 4.10; N, 16.75. Found: C, 34.45; H, 3.87; N, 16.32.

Nickel(II) (*N*-Phenyl-*N,N*-bis(1-propan-2-onyl oxime)amine) Chloride ($Ni(ABOH_2)Cl_2$). $Ni(ABOH_2)Cl_2$ was prepared similarly to $Ni(TRISOXH_3)Cl_2$ in methanol, yielding a green solid (71% yield). FTIR (KBr): 2912 (m), 1599 (m), 1497 (s), 1466 (s), 1428 (m), 1377 (m), 1221 (s), 1099 (m), 1072 (s), 1038 (m), 972 (s), 909 (m), 875 (m), 810 (m), 756 (m), 695 (m), 670 (m), 602 (m), 530 (m) cm-1. MS: $[Ni(ABOH_2)]_2Cl_3^+$ at $m/z = 693.1$ (5%), $[Ni(ABOH_1)]_2Cl^+$ at $m/z = 621.1$ (25%), $[Ni(ABOH_2)][Ni(ABOH_1)]^+$ at $m/z = 583.1$ (15%), $Ni(ABOH_2)Cl^+$ at $m/z = 328.0$ (15%), $Ni(ABOH_1)^+$ at $m/z = 292.1$ (100%).

Nickel(II) (*N,N*-Bis(1-propan-2-onyl oxime) Glycine *N*′-Methylamide) Chloride ($Ni(GLABOH_3)Cl_2$). $Ni(GLABOH_3)Cl_2$ was prepared similarly to $Ni(TRISOXH_3)Cl_2$ in methanol. Blue-green crystals (79% yield) for X-ray crystallography were obtained by slow evaporation of a methanol/ethyl acetate solution of $Ni(GLABOH_3)Cl_2$ in a test tube. FTIR (KBr): 2956 (m), 2916 (m), 1643 (vs), 1568 (m), 1459 (s), 1405 (s), 1382 (s), 1316 (m), 1272

(w), 1231 (m), 1161 (m), 1131 (m), 1052 (m), 1027 (m), 988 (m), 911 (m), 857 (m), 734 (w), 703 (m), 651 (m), 595 (m), 556 (m) cm^{-1}. MS: $Ni(GLABOH_3)Cl^+$ at $m/z = 323.0$ (100%), $Ni(GLABOH_3)(CH_3COO)^+$ at $m/z = 347.1$ (95%), $[Ni(GLABOH_2)]_2Cl^+$ at $m/z = 609.1$ (15%), $Ni(GLABOH_2)Ni(GLABOH_3)Cl_2^+$ at $m/z = 645.1$ (15%), $[Ni(GLABOH_3)]_2Cl_3$ at $m/z = 681.1$ (15%). Anal. Calcd for $Ni(C_9H_{18}N_4O_3)Cl_2$ (359.86): C, 30.05; H, 5.04; N, 15.57. Found: C, 30.15; H, 4.59; N, 15.36.

Nickel(II) (*N,N*-Bis(1-propan-2-onyl oxime) Glycine *N*′-Methylamide) Nitrate ($Ni(GLABOH_3)(NO_3)_2$). $Ni(GLABOH_3)(NO_3)_2$ was prepared similarly to $Ni(PRABOH_2)(NO_3)_2$ in methanol, yielding a blue solid (60% yield). FTIR (KBr): 2979 (m), 2931 (m), 1648 (vs), 1578 (m), 1456 (s), 1361 (vs), 1311 (s), 1229 (s), 1169 (m), 1135 (m), 1110 (w), 1083 (m), 1048 (s), 997 (m), 920 (m), 859 (m), 812 (m), 738 (w), 687 (m), 597 (m), 558 (m) cm^{-1}. MS: $Ni(GLABOH_3)NO_3^+$ at $m/z = 350.0$ (75%), $Ni(GLABOH_2)^+$ at $m/z = 287.1$ (35%).

Nickel(II) (*N,N*-Bis(1-propan-2-onyl oxime)-L-phenylalanine *N*′-Methylamide) Nitrate ($Ni(PAMBOH_3)(NO_3)_2$). $Ni(PAMBOH_3)(NO_3)_2$ was prepared similarly to $Ni(PRABOH_2)(NO_3)_2$ in methanol. Blue crystals (68% yield) for X-ray crystallography were obtained by slow diffusion of ethyl acetate into an ethanol solution of $Ni(PAMBOH_3)(NO_3)_2$ in a test tube. FTIR (KBr): 1737 (m), 1629 (s), 1550 (m), 1384 (s), 1304 (s), 1157 (m), 1043 (s), 861 (m), 827 (m), 756 (m), 702 (m), 537 (m) cm^{-1}. MS: $[Ni(PAMBOH_2)]_2NO_3^+$ at $m/z = 816$ (25%), $Ni(PAMBOH_2)Ni(PAMBOH_1)^+$ at $m/z = 753$ (15%), $Ni(PAMBOH_3)NO_3^+$ at $m/z = 440$ (100%). Anal. Calcd for $Ni(C_{16}H_{24}N_4O_3)(NO_3)_2 \cdot 0.25\ CH_3COOCH_2CH_3 + 1.25H_2O$ (547.64): C, 37.29; H, 5.25; N, 15.35. Found: C, 36.96; H, 5.01; N, 14.86.

Nickel(II) (*N,N*-Bis(1-propan-2-onyl oxime)-L-phenylalanine *N*′-Methylamide) Chloride ($Ni(PAMBOH_3)Cl_2$). $Ni(PAMBOH_3)Cl_2$ was prepared similarly to $Ni(TRISOXH_3)Cl_2$ in methanol, yielding a blue solid (74% yield). FTIR (KBr): 1625 (vs), 1554 (w), 1447 (m), 1410 (m), 1382 (m), 1237 (w), 1156 (w), 1066 (m), 859 (w), 748 (m), 687 (s), 553 (s) cm^{-1}. MS: $[Ni(PAMBOH_3)]_2Cl_3^+$ at $m/z = 861$ (25%), $Ni(PAMBOH_3)Cl^+$ at $m/z = 413$ (100%).

Nickel(II) (*N,N*-Bis(1-acetophenone oxime)-L-phenylalanine *N*′-Methylamide) Chloride ($Ni(PAMABPOH_3)Cl_2$). $Ni(PAMABPOH_3)Cl_2$ was prepared similarly to $Ni(TRISOXH_3)Cl_2$ in methanol. Blue-green crystals (79% yield) for X-ray crystallography were obtained by slow diffusion of diethyl ether into a 50/50 methanol/ethanol solution of $Ni(PAMABPOH_3)Cl_2$ in a test tube. FTIR (KBr): 2932 (m), 1620 (vs), 1550 (m), 1433 (s), 1288 (m), 1253 (m), 1162 (m), 1057 (s), 1026 (s), 841 (w), 760 (m), 687 (s), 567 (m), 534 (m) cm^{-1}. MS: $Ni(PAMABPOH_3)Cl^+$ at $m/z = 537$ (100%). Anal. Calcd for $Ni(C_{26}H_{28}N_4O_3)Cl_2 \cdot 1H_2O$ (592.14): C, 52.74; H, 5.11; N, 9.46. Found: C, 52.77; H, 4.80; N, 9.30.

Nickel(II) (*N*-2-Hydroxyethyl-*N, N*-bis(1-propan-2-onyl oxime)-amine) Chloride ($Ni(EABOH_3)Cl_2$). $Ni(EABOH_3)Cl_2$ was prepared similarly to $Ni(TRISOXH_3)Cl_2$ in methanol. Blue-green crystals (72% yield) for X-ray crystallography were obtained by slow diffusion of a layer of acetone into a methanol solution of $Ni(EABOH_3)Cl_2$ in a closed flask. FTIR (KBr): 2922 (s), 1628 (m), 1462 (s), 1439 (s), 1397 (s), 1380 (s), 1303 (w), 1242 (m), 1111 (m), 1065 (s), 1034 (s), 996 (m), 968 (m), 905 (m), 873 (m), 680 (s), 626 (m), 527 (m) cm^{-1}. MS: $Ni(EABOH_3)Cl^+$ at $m/z = 296$ (100%), $Ni(EABOH_2)^+$ at $m/z = 260$ (35%). Anal. Calcd for $Ni(C_8H_{17}N_3O_3)Cl_2$ (332.84): C, 28.87; H, 5.15; N, 12.62. Found: C, 29.03; H, 4.79; N, 12.57.

Nickel(II) (*N*-2-Hydroxyethyl-*N,N*-bis(1-propan-2-onyl oxime)-amine) Nitrate ($Ni(EABOH_3)(NO_3)_2$). $Ni(EABOH_3)(NO_3)_2$ was prepared similarly to $Ni(PRABOH_2)(NO_3)_2$ in methanol, yielding a purple solid (45% yield). FTIR (KBr): 2920 (m), 1472 (s), 1458 (s), 1431 (s), 1383 (vs), 1333 (s), 1291 (s), 1244 (m), 1236 (m), 1106 (m), 1069 (m), 1040 (m), 997 (w), 967 (w), 904 (m), 877 (m), 815 (m), 683 (m), 661 (m) cm^{-1}. MS: $Ni(EABOH_3)NO_3^+$ at $m/z = 323$ (65%).

Nickel(II) (*N*-(Pyridin-2-yl)methyl-*N,N*-bis(1-propan-2-onyl oxime)amine) Chloride ($Ni(PYRABOH_2)Cl_2$). $Ni(PYRABOH_2)Cl_2$ was prepared similarly to $Ni(TRISOXH_3)Cl_2$ in methanol. Blue crystals (66% yield) for X-ray crystallography were obtained by slow evaporation of a ethanol/methanol solution of $Ni(PYRABOH_2)Cl_2$ in a closed flask. FTIR (KBr): 2929 (m), 1667 (w), 1608 (m), 1574 (w), 1467 (s), 1437 (s), 1379 (s), 1314 (m), 1287 (m), 1235 (m), 1162 (w), 1125 (m), 1107 (m), 1060 (s), 1032 (s), 995 (m), 926 (m), 864 (m), 851 (m), 773 (s), 741 (w), 673 (m), 602 (m), 540 (m), 513 (m) cm^{-1}. MS: $Ni(PYRABOH_2)Cl^+$ at $m/z = 343.0$ (100%). Anal. Calcd for $Ni(C_{12}H_{18}N_4O_2)Cl_2$ (379.90): C, 37.94; H, 4.78; N, 14.75. Found: C, 37.66; H, 4.65; N, 14.90.

Nickel(II) (*N*-(Pyridin-2-yl)methyl-*N,N*-bis(1-propan-2-onyl oxime)amine) Nitrate ($Ni(PYRABOH_2)(NO_3)_2$). $Ni(PYRABOH_2)(NO_3)_2$ was prepared similarly to $Ni(PRABOH_2)(NO_3)_2$ in methanol. Purple crystals (82% yield) were obtained by slow diffusion of a layer of ethyl acetate into a methanol solution of $Ni(PYRABOH_2)(NO_3)_2$ in a closed flask. FTIR (KBr): 2923 (m), 1608 (m), 1470 (s), 1449 (s), 1384 (vs), 1326 (s), 1241 (m), 1159 (w), 1105 (w), 1067 (m), 1048 (m), 1025 (m), 998 (w), 922 (w), 889 (w), 867 (w), 852 (w), 770 (m), 737 (w), 673 (w) cm^{-1}. MS: $Ni(PYRABOH_1)Ni(PYRABO)^+$ at $m/z = 613$ (60%), $Ni(PYRABOH_2)NO_3^+$ at $m/z = 370$ (100%).

Nickel(II) (*N,N*-Bis(1-propan-2-onyl oxime)glycinate) Chloride ($Ni(GLYBOH_2)Cl$). Potassium *N,N*-bis(1-propan-2-onyl oxime)-glycinate (0.20 g, 7.8×10^{-4} mol) ($GLYBOH_2K$) and 0.19 g (8.0×10^{-4} mol) of nickel(II) chloride hexahydrate were combined in 15 mL of methanol and stirred to yield a blue solution, which was reduced in volume by slow evaporation in a test tube. KCl precipitate was filtered from the solution, and further evaporation yielded a blue solid (39% yield). FTIR (KBr): 2925 (m), 1590 (vs), 1431 (s), 1403 (s), 1325 (m), 1290 (w), 1235 (m), 1124 (w), 1067 (m), 1034 (m), 995 (w), 926 (w), 895 (w), 858 (w), 731 (m), 680 (m) cm^{-1}. MS: $Ni(GLYBOH_2)Ni(GLYBOH_1)^+$ at $m/z = 547.1$ (100%).

Nickel(II) (*N,N*-Bis(1-propan-2-onyl oxime)glycinate) Nitrate ($Ni(GLYBOH_2)NO_3$). $Ni(GLYBOH_2)NO_3$ was prepared similarly to $Ni(GLYBOH_2)Cl$, using acetonitrile as the solvent and filtering off KNO_3 precipitate to yield a blue solid (32% yield). FTIR (KBr): 2930 (m), 1606 (s), 1382 (vs), 1357 (vs), 1234 (m), 1120 (w), 1071 (m), 1035 (m), 996 (w), 930 (w), 896 (w), 826 (m), 737 (m), 678 (m) cm^{-1}. MS: $Ni(GLYBOH_2)Ni(GLYBOH_1)^+$ at $m/z = 547.1$ (100%), $Ni(GLYBOH_2)^+$ at $m/z = 274.0$ (65%).

Experimental Methods. NMR spectra were obtained using a Bruker AC250 spectrometer as d_6-DMSO, $CDCl_3$, d_6-acetone, or D_2O solutions and referenced to TMS (or CH_3OH for ^{13}C NMR spectra in D_2O solutions). FTIR spectra were collected on a Bio-Rad Excalibur spectrometer as KBr pellets. UV−vis absorption spectra were collected on a Hewlett-Packard 8453 spectrometer using a 2 cm path length cell as H_2O, CH_3OH, or CH_3CN solutions. Circular dichroism spectra were collected on a Jasco J-715 spectropolarimeter (interfaced with a PC) using a 2 cm path length cell as DMF solutions. Mass spectra were collected by the University of Cincinnati Mass Spectrometry Facility on a Micromass QTOF-II or an IonSpec FT-ICR mass spectrometer with electrospray sample introduction. Samples were prepared by dissolution in CH_3OH, with NaCl added to neutral ligands to induce charge in some cases. Magnetic susceptibility data of solid samples

ground to a fine powder were collected at room temperature using a Johnson Matthey MSB-1 balance, which was calibrated with a powder sample of recrystallized $HgCo(SCN)_4$. Elemental analyses (CHN) of all samples were performed by Quantitative Technologies, Inc. (Whitehouse, NJ). Samples submitted for CHN analysis were crystalline solids prepared similarly to X-ray crystallographic samples and were ground to a powder and dried under vacuum before submission for CHN analysis.

X-ray Crystallography. Intensity data for $Ni(GLABOH_3)Cl_2$, $Ni(PRABOH_2)(NO_3)_2$, $Ni(PAMABPOH_3)Cl_2$, $[Ni(PEABOH_2)Cl]_2(\mu\text{-}Cl)_2$, $Ni(TRISOXH_3)Cl_2$, and $Ni(ABOH_2)(NO_3)_2$ were collected at 150 K on a standard SMART 1K CCD diffractometer using graphite-monochromated Mo Kα radiation, $\lambda = 0.71073$ Å, while $Ni(PAMBOH_3)(NO_3)_2$ was collected at 298 K. The detector was set at a distance of 4.5−5.0 cm from the crystal. A series of 10−30 s data frames measured at 0.3° increments of ω were collected to calculate a unit cell. For data collection, frames were measured for a duration of 10−30 s at 0.3° intervals of ω, with a maximum θ value of approximately 28°.

Intensity data for $Ni(PYRABOH_2)Cl_2$ and $Ni(EABOH_3)Cl_2$ were collected at 150 K on a standard SMART 6000 CCD diffractometer using graphite-monochromated Mo Kα radiation, $\lambda = 0.71073$ Å, while $[Ni(OBOH_2)Cl]_2(\mu\text{-}Cl)_2$ was collected at 295 K. The detector was set at a distance of 4.5−6.5 cm from the crystal. A series of 20−30 s data frames measured at 0.3° increments of ω were collected to calculate a unit cell. For data collection, frames were measured for a duration of 20−35 s at 0.3° intervals of ω, with a maximum θ value ranging from 28 to 32°.

Intensity data for $[Ni(PRABOH_2)Cl]_2(\mu\text{-}Cl)_2$ were collected at 150 K on a standard SMART 2K CCD diffractometer using graphite-monochromated Ag Kα radiation, $\lambda = 0.56086$ Å. The detector was set at a distance of 5 cm from the crystal. A series of 20 s data frames measured at 0.3° increments of ω were collected to calculate a unit cell. For data collection, frames were measured for a duration of 20 s at 0.3° intervals of ω, with a maximum θ value of 21.94°. The data frames were processed using the program SAINT.[10] The data were corrected for decay, Lorentz, and polarization effects. An absorption correction based on the multiscan technique and beam corrections were applied using SADABS.[10]

The structures were solved by a combination of direct methods or Patterson (SHELXTL[10]) and the difference Fourier technique and refined by full-matrix least squares on F^2. Non-hydrogen atoms were refined with anisotropic displacement parameters. Weights were assigned as $w^{-1} = [\sigma^2(F_o^2) + (aP)^2 + bP]$ where $P = 0.33333F_o^2 + 0.66667F_c^2$. Hydrogen atoms were either located directly from the difference map or calculated based on geometric criteria. −OH or −NH hydrogens were held fixed where located. All remaining hydrogens were treated with a riding model in subsequent refinements. The isotropic temperature factors for the H-atoms were defined as $U(H) = aU_{eq}$ of the adjacent atom where $a = 1.5$ for $-CH_3$ and −OH and 1.2 for all others. In the case of $Ni(TRISOXH_3)Cl_2$, all hydrogens were located directly and the positions and U_{iso} refined.

Methyl groups are disordered in $Ni(GLABOH_3)Cl_2$ and $Ni(TRISOXH_3)Cl_2$, the hydrogen occupancies were set at 0.5. Several atoms in $Ni(PAMBOH_3)(NO_3)_2$ (O9, C10, C11, and C12) have large displacement parameters indicative of disorder; their displacement parameters were set to be equivalent to their better behaved neighbors (O8, C9, and C11). The large displacement parameter for C14 was left where it refined. The ethyl acetate solvent of crystallization occupancy was set at 0.5 for $Ni(PAMBOH_3)(NO_3)_2$. The disorder in the displacement parameters was left where refined, since a suitable disorder model was not realized. $Ni(PAMABOH_3)Cl_2$ crystallized as an ethanol solvate. Two molecules of acetone crystallize in the lattice of $Ni(ABOH_2)(NO_3)_2$. Some disorder is observed, but separation of conformers was not achieved. Two molecules of water are present in the lattice for $Ni(PYRABOH_2)Cl_2$. Additionally, some disorder is observed for C2−C5, as indicated by the enlarged displacement parameters, but these were left where they refined. The octyl group in $[Ni(OBOH_2)Cl]_2(\mu\text{-}Cl)_2$ shows disorder. The anisotropic displacement parameter for C14 was held equivalent to C13. The PRABO ligand in $[Ni(PRABOH_2)Cl_2](\mu\text{-}Cl)_2$ is disordered in both the backbone, C1, and the propyl group, C9. The refined occupancies for the major conformer of C1 and C9 are 53% and 54%, respectively. The refinement converged smoothly with crystallographic agreement factors as given in Tables 1−3.

Results and Discussion

Ligand Synthesis. The synthesis of the general bis(oxime) tripodal amine ligand is achieved by reaction of the oxime-containing alkylation reagent TACO[5] with a primary amine containing the third donor "arm" of choice (Scheme 1). This synthetic method allows for facile isolation of pure ligands, as is evidenced in the ^{1}H NMR spectra, with incorporation of nearly any functional group into the bis(oxime) tripodal amine ligand framework. Ligands reported here include a variety of noncoordinating, weakly coordinating, and strongly coordinating functional groups on the third arm of the tripod. The ligands $PRABOH_2$, $PEABOH_2$, $OBOH_2$, and $ABOH_2$ all contain noncoordinating third arms. Ligands such as $GLABOH_3$, $PAMBOH_3$, and $PAMABPOH_3$ can provide a weakly coordinating donor group such as an amide oxygen. $EABOH_3$, $GLYBOH_2^-$, $PYRABOH_2$, and $TRISOXH_3$ provide stronger donor groups such as alcohol, carboxylate, pyridyl, and oxime groups, respectively (Figure 1).

In addition to variability in the donor set, this facile synthetic method allows for incorporation of other structural features into the ligands and complexes. Chirality can be introduced by the use of natural amino acids as the primary amine starting materials. Chiral metal complexes offer several advantages over their nonchiral counterparts, such as the possibility of catalyzing stereospecific reactions[11] and the availability of circular dichroism (CD) spectroscopy as an additional tool for the characterization of the complexes and their reactivity. We have previously reported the chiral L-methionine based MABO ligand (along with its nickel(II) and zinc(II) complexes),[12] and two ligands based on L-phenylalanine, $PAMBOH_3$, and $PAMABPOH_3$ are reported here. With $PAMABPOH_3$, the capability to change the steric and solubility properties of the oxime donor arms is also

(10) (a) SMART and SAINT programs were used for data collection and data processing (Siemens Analytical X-ray Instruments, Inc., Madison, WI). (b) SADABS was used for the application of semiempirical absorption and beam corrections (G. M. Sheldrick, University of Goettingen, Germany, 1996). (c) SHELXTL was used for the structure solution and generation of figures and tables (G. M. Sheldrick, University of Goettingen, Germany and Siemens Analytical X-ray Instruments, Inc., Madison, WI).

(11) Palucki, M.; Finney, N. S.; Pospisil, P. J.; Güler, M. L.; Ishida, T.; Jacobsen, E. N. *J. Am. Chem. Soc.* **1998**, *120*, 948−954.

(12) Rosa, D. T.; Krause Bauer, J. A.; Baldwin, M. J. *Inorg. Chem.* **2001**, *40*, 1606.

Table 1. X-ray Crystallography Parameters and Factors for the Complexes $Ni(TRISOXH_3)Cl_2$, $Ni(PYRABOH_2)Cl_2$, $Ni(EABOH_3)Cl_2$, $Ni(GLABOH_3)Cl_2$, and $Ni(PAMABPOH_3)Cl_2$

	$Ni(TRISOXH_3)Cl_2$	$Ni(GLABOH_3)Cl_2$	$Ni(PYRABOH_2)Cl_2$	$Ni(EABOH_3)Cl_2$	$Ni(PAMABPOH_3)Cl_2$
emp form	$C_9H_{18}Cl_2N_4O_3Ni$	$C_9H_{18}Cl_2N_4O_3Ni$	$C_{12}H_{18}Cl_2N_4O_2Ni\cdot 2H_2O$	$C_8H_{17}Cl_2N_3O_3Ni$	$C_{26}H_{28}Cl_2N_4O_3Ni\cdot C_2H_6O$
fw	359.88	359.88	415.95	332.86	620.20
temp (K)	150(2)	150(2)	150(2)	150(2)	150(2)
crystal system	monoclinic	monoclinic	orthorhombic	monoclinic	monoclinic
space group	$P2_1/n$	$P2_1$	$P2_12_12_1$	$P2_1/n$	$P2_1$
unit cell dimens					
a (Å)	8.9006(4)	8.094(3)	8.0043(2)	8.4430(3)	7.9618(3)
b (Å)	18.2483(8)	11.710(3)	14.7734(3)	12.1399(4)	16.6749(6)
c (Å)	8.9406(4)	8.319(2)	14.9036(3)	12.8157(4)	11.0062(4)
α (deg)	90	90	90	90	90
β (deg)	94.357(1)	114.982(14)	90	91.081(1)	100.2490(10)
γ (deg)	90	90	90	90	90
vol ($Å^3$), *Z*	1447.94(11), 4	714.7(3), 2	1762.36(7), 4	1313.34(8), 4	1437.89(9), 2
density (calcd) (Mg/m^3)	1.651	1.672	1.568	1.683	1.432
abs coeff (mm^{-1})	1.717	1.740	1.427	1.884	0.901
Flack param	N/A	0.055(10)	0.013(9)	N/A	0.018(11)
final *R* indices [$I > 2\sigma(I)$]					
R1	0.0295	0.0248	0.0337	0.0305	0.0366
wR2	0.0685	0.0579	0.0691	0.0757	0.0917
R indices (all data)					
R1	0.0332	0.0272	0.0362	0.0339	0.0429
wR2	0.0699	0.0586	0.0699	0.0773	0.0949

Table 2. X-ray Crystallography Parameters and Factors for the Complexes $Ni(PAMBOH_3)(NO_3)_2$, $Ni(ABOH_2)(NO_3)_2$, and $Ni(PRABOH_2)(NO_3)_2$

	$Ni(PAMBOH_3)(NO_3)_2$	$Ni(PRABOH_2)(NO_3)_2$	$Ni(ABOH_2)(NO_3)_2$
emp form	$C_{16}H_{24}N_6O_9Ni\cdot {}^1/_2\,(C_4H_8O_2)$	$C_9H_{19}N_5O_8Ni$	$C_{12}H_{17}N_5O_8Ni\cdot 2\,(C_3H_6O)$
fw	547.17	384.00	534.17
temp (K)	298(2)	150(2)	150(2)
crystal system	orthorhombic	monoclinic	monoclinic
space group	$P2_12_12_1$	$P2_1/n$	$P2_1/n$
unit cell dimens			
a (Å)	12.727(2)	8.3181(2)	12.0935(8)
b (Å)	12.970(2)	19.4089(5)	15.3388(10)
c (Å)	16.683(2)	9.9222(1)	13.7565(9)
α (deg)	90	90	90
β (deg)	90	94.897(1)	106.808(1)
γ (deg)	90	90	
vol ($Å^3$), *Z*	2753.8(7), 4	1596.04(6), 4	2442.8(3), 4
dens (calcd) (Mg/m^3)	1.320	1.598	1.452
abs coeff (mm^{-1})	0.761	1.264	0.854
Flack paramr	0.00(2)	N/A	N/A
final *R* indices [$I > 2\sigma(I)$]			
R1	0.0637	0.0342	0.0647
wR2	0.1479	0.0839	0.1100
R indices (all data)			
R1	0.1559	0.0457	0.0763
wR2	0.2048	0.0884	0.1132

shown, as the typical methyl groups of most of the ligands in the series are replaced by phenyl groups. The acetophenone-based reagent TABO, similar to TACO, provides an easy method for addition of oxime donor arms with phenyl groups to amines. While incorporation of the third donor arm can be easily achieved by choice of the amine starting material, addition of carboxylate donor groups by reaction of amino acids with TACO does not proceed as easily, likely due to relatively low nucleophilicity of the zwitterion form of the amino acids. This problem can be overcome by conversion of the amino acid to its ester derivative, followed by reaction with TACO to give the ester bis(oxime) tripodal amine and then saponification of the ester with KOH to give the potassium carboxylate salt.

Synthesis and Structure of Ni(II) Complexes. The nickel(II) complexes of this series of polyoxime tripodal amine ligands can be easily obtained by addition of 1 equiv of the ligand to the Ni(II) salt of choice, followed by crystallization from a variety of high and medium polarity solvents. With the exception of the $GLYBOH_2K$ ligand, at least one X-ray crystal structure of a Ni(II) complex has been obtained for each ligand. In these crystal structures, the polydentate ligands all bind in a manner similar to nickel(II), with the oxime nitrogens and the central amine forming a general N_3 donor unit, which always coordinates in a facial mode. The third arm may or may not provide additional donor atoms, depending on the type of functional group on that arm. All of these complexes have six-coordinate, pseudo-octahedral geometry at the nickel center, with similar Ni−N(amine) and Ni−N(oxime) bond lengths and N−Ni−N bond angles for the common bis(oxime)amine N_3 donor set (Table 4). However, some notable differences in structure result from both the nature of the ligand's third arm and the anion of the Ni(II) salt which is used. Three major crystal structure types are observed in the Ni(II) complexes of this series of ligands. (Type 1) For the tetradentate ligands

Table 3. X-ray Crystallography Parameters and Factors for the Complexes $[Ni(PRABOH_2)Cl]_2(\mu\text{-}Cl)_2$, $[Ni(PEABOH_2)Cl]_2(\mu\text{-}Cl)_2$, and $[Ni(OBOH_2)Cl]_2(\mu\text{-}Cl)_2$

	$[Ni(PRABOH_2)Cl]_2(\mu\text{-}Cl)_2$	$[Ni(PEABOH_2)Cl]_2(\mu\text{-}Cl)_2$	$[Ni(OBOH_2)Cl]_2(\mu\text{-}Cl)_2$
emp form	$C_{18}H_{38}Cl_4N_6O_4Ni_2$	$C_{28}H_{42}Cl_4N_6O_4Ni_2$	$C_{28}H_{58}Cl_4N_6O_4Ni_2$
fw	661.76	785.90	802.02
temp (K)	150(2)	150(2)	295(2)
crystal system	monoclinic	triclinic	monoclinic
space group	$P2_1/n$	P-1	$C2/c$
unit cell dimens			
a (Å)	8.5525(3)	8.4695(2)	23.8527(1)
b (Å)	15.9383(6)	10.2688(3)	14.0684(6)
c (Å)	10.5236(4)	10.5412(2)	11.7874(5)
α (deg)	90	111.407(1)	90
β (deg)	103.847(1)	100.985(1)	90.715(1)
γ (deg)	90	94.575(1)	90
vol (Å^3), Z	1392.81(9), 2	826.64(3), 1	3955.2(3), 4
density (calcd) (Mg/m^3)	1.578	1.579	1.347
abs coeff (mm^{-1})	0.923	1.506	1.260
Flack param	N/A	N/A	N/A
final R indices [$I > 2\sigma(I)$]			
R1	0.0459	0.0234	0.0595
wR2	0.1074	0.0589	0.1205
R indices (all data)			
R1	0.0783	0.0285	0.0776
wR2	0.1162	0.0602	0.1278

Scheme 1. General Reaction Scheme for the Synthesis of Bis(oxime) Tripodal Amine Ligands

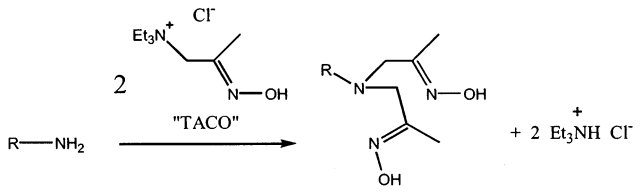

($TRISOXH_3$, $GLABOH_3$, $PAMBOH_3$, $PAMABPOH_3$, $EABOH_3$, and $PYRABOH_2$), monomeric, six-coordinate, pseudo-octahedral geometries are observed (Figure 2 and Figure 3). In these structures, the two "free" nickel coordination positions are occupied by monodentate anions (NO_3^- or Cl^-) (In previously reported structures of these types, solvent molecules may coordinate in the place of nitrate anions.[4,12]) (Type 2) For the tridentate ligands ($ABOH_2$, $OBOH_2$, $PEABOH_2$, and $PRABOH_2$), the complexes with $Ni^{II}(NO_3)_2$ form monomeric, pseudo-octahedral structures (Figure 4). The coordination sphere of the nickel is completed by one nitrate anion acting as a bidentate ligand in the two free equatorial positions and a second nitrate acting as a monodentate ligand in the free axial position (defined as trans to the amine donor). (Type 3) For the same tridentate ligands with $Ni^{II}Cl_2$, bis(μ-Cl) bridged dimers are formed, in which the neighboring chlorides fill the coordination sphere of the nickel (Figure 5). There are multiple examples, with no exceptions, of each crystal structure type, strongly indicating that these are generalized structural phenomena controlled by both the ligand donor set and coordination properties of the anions in the complex. Thus, of the complexes which have not been structurally characterized by X-ray crystallography, it might be expected that $Ni(GLABOH_3)(NO_3)_2$, $Ni(PAMBOH_3)Cl_2$, $Ni(PYRABOH_2)(NO_3)_2$, and $Ni(EABOH_3)(NO_3)_2$ will assume structure type 1, $Ni(PEABOH_2)(NO_3)_2$ and $Ni(OBOH_2)(NO_3)_2$ will assume structure type 2, and $Ni(ABOH_2)Cl_2$ will assume structure type 3. The $Ni(GLYBOH_2)Cl$ and $Ni(GLYBOH_2)(NO_3)$ complexes, with their tetradentate N_3O donor set, may be

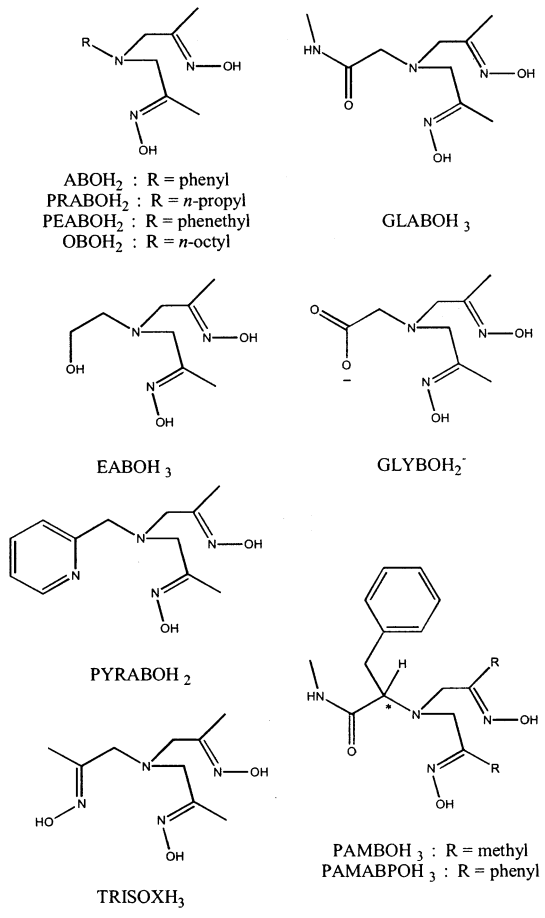

Figure 1. Library of tripodal amine ligands containing at least two oxime donor groups.

expected to form structures of type 1. However, the negative charge of the $GLYBOH_2^-$ ligand will likely result in the coordination of only one anion, with solvent occupying the sixth coordination position. Also, it is conceivable that the carboxylate donor arm could bridge to other metal centers, forming dimeric structures. Room-temperature magnetic

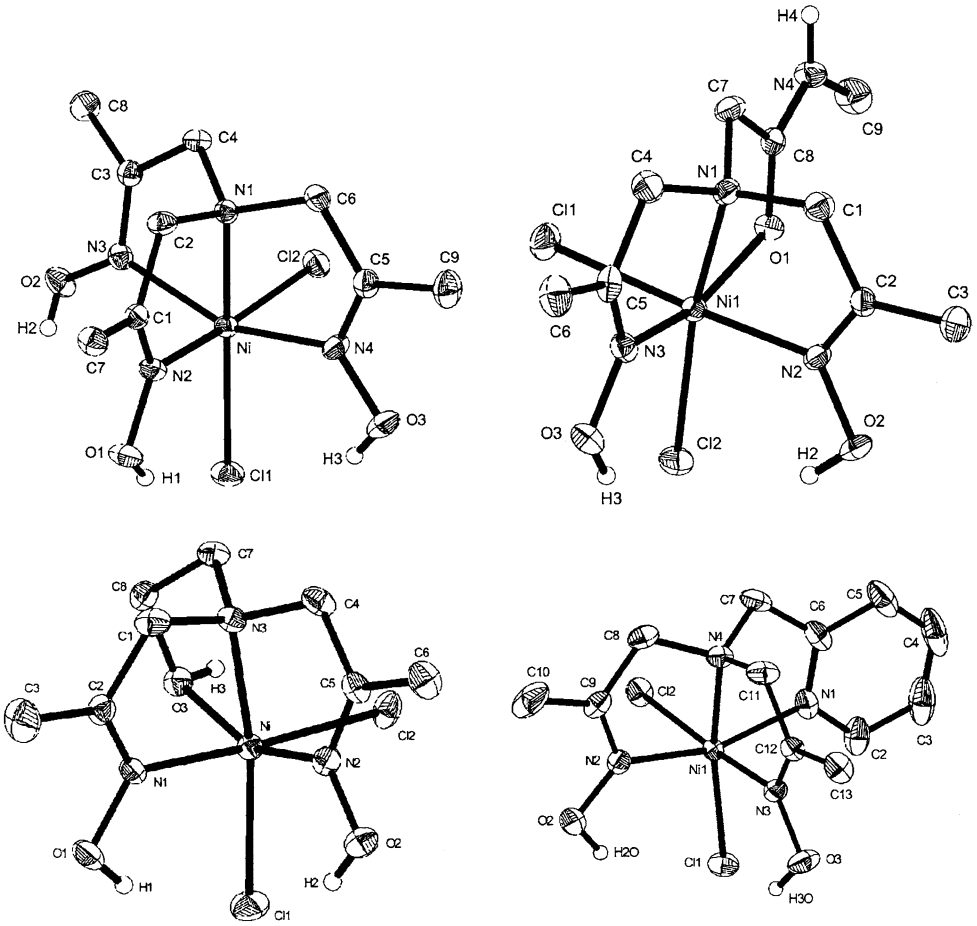

Figure 2. X-ray crystal structures (ORTEP views) of Ni(TRISOXH$_3$)Cl$_2$ (top left), Ni(GLABOH$_3$)Cl$_2$ (top right), Ni(EABOH$_3$)Cl$_2$ (bottom left), and Ni(PYRABOH$_2$)Cl$_2$ (bottom right). These tetradentate ligands form six-coordinate, monomeric complexes with Ni(II).

Table 4. X-ray Crystallographic Nickel−Ligand Bond Lengths

	bond lengths (Å)			
complex	Ni−N(oxime)	Ni−N(amine)	Ni−(third arm)	bond type
Ni(TRISOXH$_3$)(NO$_3$)$_2$ (ref 4)	2.051(2) 2.099(2)	2.085(2)	2.078(2)	Ni−N(oxime)
Ni(TRISOXH$_3$)Cl$_2$	2.0485(14) 2.0957(14)	2.1131(13)	2.0367(14)	Ni−N(oxime)
Ni(PYRABOH$_2$)Cl$_2$	2.1198(15) 2.0628(15)	2.1110(15)	2.0811(16)	Ni−N(pyridyl)
Ni(EABOH$_3$)Cl$_2$	2.0410(12) 2.0496(12)	2.1189(12)	2.1565(10)	Ni−O(alcohol)
Ni(GLABOH$_3$)Cl$_2$	2.062(2) 2.034(2)	2.115(2)	2.069(2)	Ni−O(amide)
Ni(PAMABPOH$_3$)Cl$_2$	2.050(2) 2.030(2)	2.140(2)	2.062(2)	Ni−O(amide)
Ni(PAMBOH$_3$)(NO$_3$)$_2$	2.024(5) 2.061(5)	2.134(5)	2.062(4)	Ni−O(amide)
[Ni(PRABOH$_2$)Cl]$_2$(μ-Cl)$_2$	2.042(3) 2.060(3)	2.186(3)	n/a	
[Ni(PEABOH$_2$)Cl]$_2$(μ-Cl)$_2$	2.0429(12) 2.0584(12)	2.2068(12)	n/a	
[Ni(OBOH$_2$)Cl]$_2$(μ-Cl)$_2$	2.040(3) 2.044(3)	2.201(3)	n/a	
Ni(PRABOH$_2$)(NO$_3$)$_2$	1.9917(17) 2.0311(16)	2.1088(17)	n/a	
Ni(ABOH$_2$)(NO$_3$)$_2$	2.011(2) 2.024(3)	2.168(2)	n/a	

susceptibility measurements for all of the nickel(II) complexes reported here are consistent with values for six-coordinated, pseudo-octahedral nickel(II).[13] Values of μ_{eff} measured for the complexes range from 2.62 to 3.33 ($\mu_{\text{spin only}} = 2.83$), which are in agreement with a spin of $S = 1$ at the metal center (See Table S1 in the Supporting Information).

The crystal structures of the nickel(II) complexes show that the hydrogens from one or more of the oxime hydroxyl

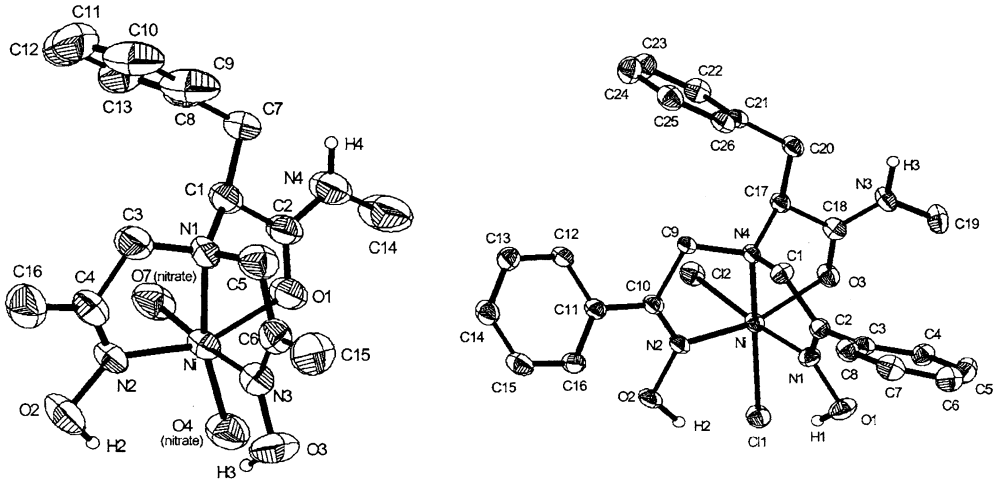

Figure 3. X-ray crystal structures (ORTEP views) of Ni(PAMBOH$_3$)(NO$_3$)$_2$ (left, noncoordinating nitrate atoms omitted for clarity) and Ni(PAMABPOH$_3$)-Cl$_2$ (right). As with the other tetradentate ligands, six-coordinate, monomeric complexes are formed. In addition, these L-phenylalanine derived ligands incorporate a chiral center into the complex, which allows for the use of CD spectroscopy.

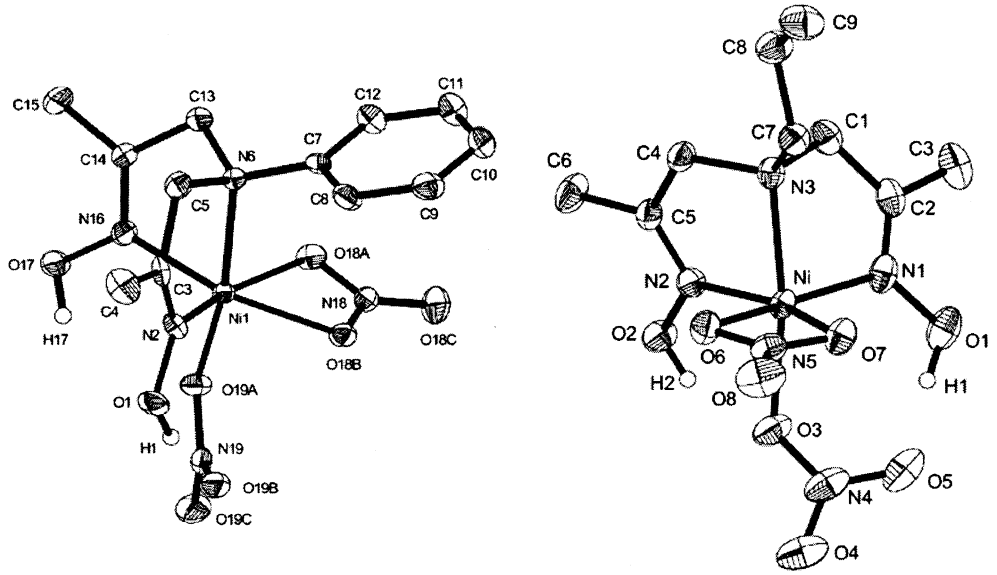

Figure 4. X-ray crystal structures (ORTEP views) of Ni(ABOH$_2$)(NO$_3$)$_2$ (left) and Ni(PRABOH$_2$)(NO$_3$)$_2$ (right). The tridentate ligands form six-coordinate, monomeric complexes when bound to Ni^{II}(NO$_3$)$_2$.

groups form intramolecular hydrogen bonds with the anion bound to the nickel center in the axial position. For example, in the crystal structure of Ni(TRISOXH$_3$)Cl$_2$ (see Figure 2), H1 and H3 of two of the oxime groups form hydrogen bonds to the axial chloride (Cl1) with distances of 2.35(3) and 2.50(3) Å, respectively. The ability of these polyoxime ligands to form hydrogen bonds with ligands or substrates bound to the metal center may provide stabilization of otherwise reactive species or enhanced reactivity with substrates. Similar intramolecular hydrogen bonding effects have been designed into polydentate ligands by others. Berreau and co-workers have reported a zinc complex in which the ligand forms a hydrogen bond to a coordinated methanol or DMF molecule as a structural model for liver alcohol dehydrogenase.[14] Similarly, Borovik and co-workers have shown that tripodal amine ligands with urea type donor groups can form hydrogen bonds to stabilize terminal hydroxide ligands in various metal complexes.[15] Metal-bound active oxygen intermediates may also be activated by hydrogen bonding, as is suggested for the vanadium haloperoxidases. Vanadium−peroxo complexes of tripodal and bipodal amine ligands reported by Butler and co-workers show intramolecular hydrogen bonds between the ligands and the metal-bound peroxide.[16] Thus, these polydentate ligands containing oxime groups may be useful for designing metal complexes with the strong potential for hydrogen bonding with and stabilization of exogenous ligands.

UV−vis Spectroscopic Characterization. The UV−vis absorption spectra of the series of tripodal amine-containing

(13) Cotton, F. A.; Wilkinson, G.; Murillo, C. A.; Bochmann, M. In *Advanced Inorganic Chemistry*, 6th ed.; John Wiley and Sons: New York, 1999; pp 838−839.

(14) (a) Garner, D. K.; Allred, R. A.; Tubbs, K. J.; Arif, A. M.; Berreau, L. M. *Inorg. Chem.* **2002**, *41*, 3533−3541. (b) Berreau, L. M.; Makowska-Grzyska, M. M.; Arif, A. M. *Inorg. Chem.* **2001**, *40*, 2212−2213.

(15) Macbeth, C. A.; Hammes, B. S.; Young, V. G.; Borovik, A. S. *Inorg. Chem.* **2001**, *40*, 4733−4741.

(16) Kimblin, C.; Bu, X.; Butler, A. *Inorg. Chem.* **2002**, *41*, 161−163.

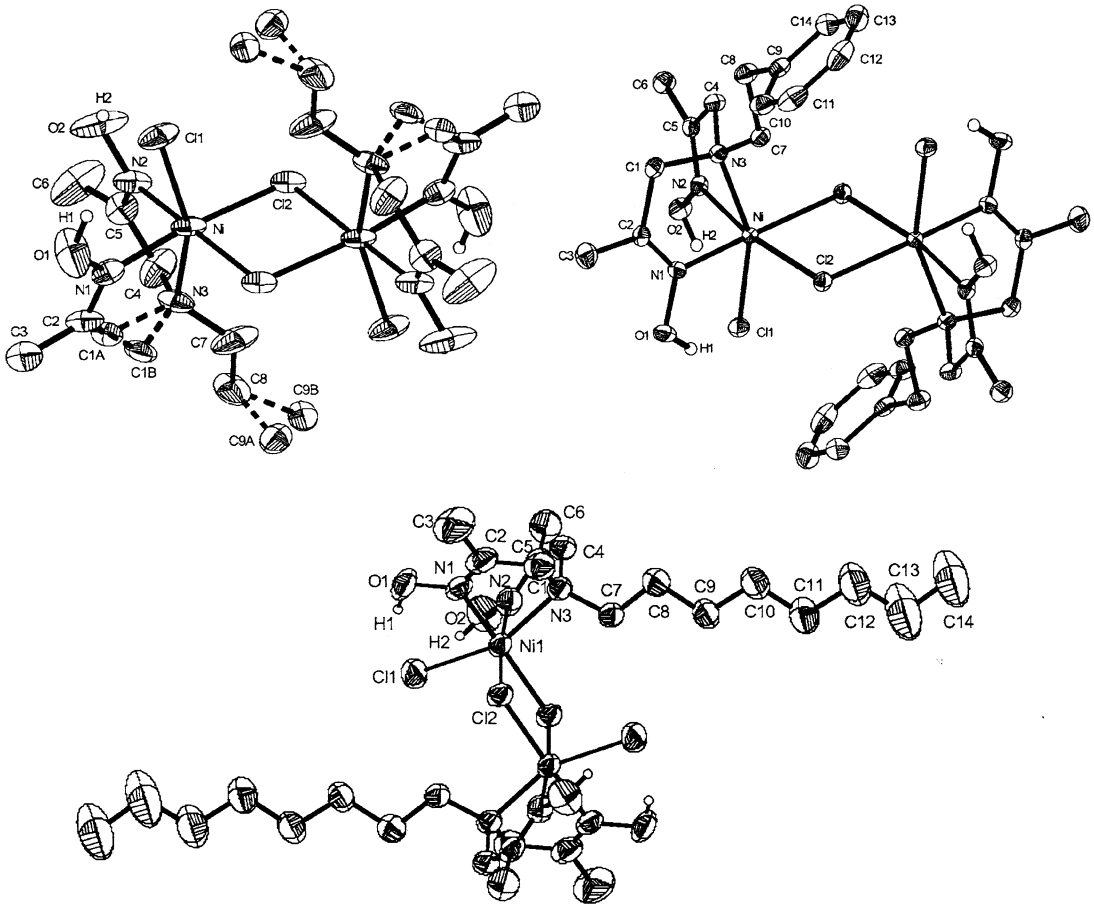

Figure 5. X-ray crystal structures (ORTEP views) of $[Ni(PRABOH_2)Cl]_2(\mu\text{-}Cl)_2$ (top left), $[Ni(PEABOH_2)Cl]_2(\mu\text{-}Cl)_2$ (top right), and $[Ni(OBOH_2)Cl]_2(\mu\text{-}Cl)_2$. The tridentate ligands, when coordinated to $Ni^{II}Cl_2$, form bis(μ-Cl) bridged dimers.

Ni(II) complexes are consistent with other six-coordinate, pseudo-octahedral Ni(II) complexes.[17] Each contains three absorption bands in the ligand field region (300−1200 nm), although for some, the highest energy of these is buried under the tail of intense high energy absorbance bands. The lowest energy transition in an octahedral d^8 complex corresponds to 10 *Dq*. The value of 10 *Dq* varies according to the nature of the third arm of the ligand, producing a reasonable spectrochemical series for the Ni(II) ligand field transitions. In acetonitrile, a relatively weakly coordinating solvent, the trend based on the third arm follows the order alkyl/aryl < amide < carboxylate < alcohol < pyridyl < oxime, which is consistent with expectations based on the donor strength of the third arm. The spectra of the nitrate salts in acetonitrile are shown in Figure 6 and values of 10 *Dq* are listed in Table 5. The value of 10 *Dq* is lower for the $ABOH_2$ complex than for complexes of the other tridentate ligands due to modulation of the donor ability of the coordinated central amine nitrogen, which is directly bound to the phenyl ring, unlike in the other aliphatic amines ($PRABOH_2$, $PEABOH_2$, $OBOH_2$).

The effects of solvent and counterions on the value of 10 *Dq* were also investigated. Complexes containing either chloride or nitrate ions were examined in methanol and water

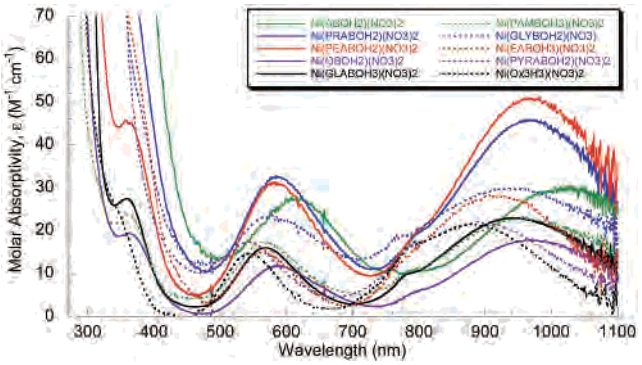

Figure 6. UV−vis absorption spectra of Ni^{II} nitrate complexes in CH_3CN solution.

(For UV−vis spectra, see Figures S1 to S4 in Supporting Information.) It appears that in water, weakly coordinating third arms (such as an amide oxygen) are displaced by the more strongly coordinating solvent molecule,[12] which slightly shifts the order of the spectrochemical series. In methanol, both the chloride and the nitrate containing complexes follow the order observed in acetonitrile. Values of 10 *Dq* for all the complexes in acetonitrile, methanol, and water are compiled in Table 5.

The spectroscopic properties of the compounds can be further explored if a chiral center is designed into the complex. Natural chiral amino acids can be used as starting

(17) Lever, A. B. P. In *Inorganic Electronic Spectroscopy*; Elsevier: Amsterdam, 1984.

Table 5. Values of 10 Dq (cm^{-1}) for the Ni(II) Complexes in Different Solvents[a]

complex	CH_3OH ($X = Cl^-$)	CH_3OH ($X = NO_3^-$)	H_2O ($X = Cl^-$)	H_2O ($X = NO_3^-$)	CH_3CN ($X = NO_3^-$)
$Ni(TRISOXH_3)X_2$	10260	10990	10990	10990	11360
$Ni(PYRABOH_2)X_2$	10200	10930	10990	10930	11240
$Ni(EABOH_3)X_2$	10100	10750	10750	10640	10870
$Ni(GLYBOH_2)X$	10000	10640	10530	10580	10640
$Ni(GLABOH_3)X_2$	9900	10420	10530	10470	10530
$Ni(PAMBOH_3)X_2$	9800	10420	10420	10310	10420
$Ni(PRABOH_2)X_2$	9430	10100	10100	10310	10310
$Ni(OBOH_2)X_2$	9760	10100	10750	10310	10200
$Ni(PEABOH_2)X_2$	9430	10100	10420	10310	10310
$Ni(ABOH_2)X_2$	< 9600	n/a	n/a	n/a	9710

[a] Complexes that are insoluble in a solvent are listed as n/a.

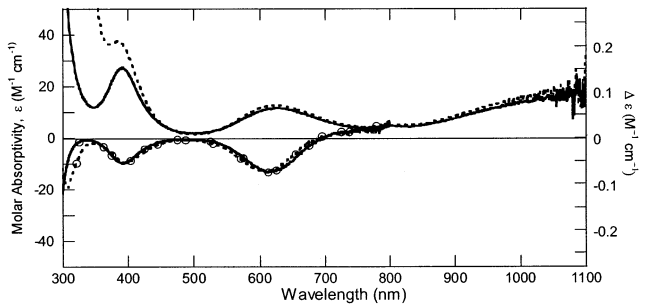

Figure 7. UV−vis (no marker) and CD (circle markers) spectra of the chiral complexes $Ni(PAMBOH_3)Cl_2$ (solid line) and $Ni(PAMABPOH_3)Cl_2$ (dashed line) in DMF.

materials in order to synthesize chiral derivatives of the tripodal amine polyoxime ligands. The metal complexes of these ligands can be probed by circular dichroism to give electronic information that is complementary to that obtained by UV−vis spectroscopy, similarly to the previously reported spectroscopic study of the Ni(II) and Zn(II) complexes of a bis(oxime) containing ligand based on L-methionine *N*′-methylamide.[12] A descent in symmetry model was used to analyze the ligand field spectra of the Ni(II) complexes, and the electronic transitions were used to examine deviations from O_h symmetry. The CD and UV−vis spectra of two new chiral complexes, $Ni(PAMBOH_3)(NO_3)_2$ and $Ni(PAMABPOH_3)(NO_3)_2$, are shown in Figure 7, demonstrating that these chiral complexes are conducive to the use of CD spectroscopy as an analytical tool in future studies of the reactivity of the complexes.

Summary and Conclusions

We have synthesized a library of novel tripodal amine ligands with at least two oxime donor groups and a variable third donor arm. Incorporation of steric and chiral features can be easily achieved without significant modification of the synthetic route. The nickel(II) complexes of these ligands have been structurally characterized by X-ray crystallography. Three generalized structure types are formed, which are determined by the ligand donor set and the anion coordination properties. In these crystal structures, interesting intramolecular hydrogen bonding is observed between the hydrogens of the oxime hydroxyl groups and the axially coordinated anions. Analysis of the UV−vis absorption spectra of this series of Ni(II) complexes shows that variance of the donor ability of the third arm of the ligand tripod can tune the ligand field energy of the metal complexes, with a spectrochemical series of alkyl/aryl < amide < carboxylate < alcohol < pyridyl < oxime for third arm donor types. It is anticipated that this variation in electronic properties and other attributes of the ligands will allow optimization of interesting reactivity for the metal complexes of these ligands.

Acknowledgment. Funding was provided by the Petroleum Research Fund administered by the American Chemical Society (ACS-PRF 37653-AC3) and the University of Cincinnati. N.K.V. was supported by NSF-REU award #CHE-0097726. Crystallographic data were collected on the SMART 1K diffractometer by J.A.K.B. through the Ohio Crystallographic Consortium located at the University of Toledo, Toledo, OH 43606 (Ohio Board of Regents 1995 Investment Fund CAP-075), and on the SMART 2K and SMART 6000 diffractometers through Dr. Alan Pinkerton, Department of Chemistry, University of Toledo, Toledo, OH. The University of Cincinnati Mass Spectrometry Facility is part of the Ohio Mass Spectrometry Consortium. We also thank Professor Apryll Stalcup at the University of Cincinnati for the use of her CD spectrometer.

Supporting Information Available: ^1H NMR, ^{13}C NMR, and mass spectra of the ligands, mass spectra of the nickel complexes, UV−vis absorption spectra of the nickel complexes in CH_3OH and H_2O, room-temperature magnetic susceptibility values, and crystallographic data in CIF format. This material is available free of charge via the Internet at http://pubs.acs.org.

IC025860Q